JOURNAL OF MATERIALS SCIENCE 24 (1989) 1439–1446

Calorimetric evaluation of the effects of SiC concentration on precipitation processes in SiC particulate-reinforced 7091 aluminium

J. L. PETTY-GALIS
Materials Analysis, Inc., Dallas, Texas 75238, USA

R. D. GOOLSBY
Mechanical Engineering Department, University of Texas at Arlington, Arlington, Texas 76019, USA

A comprehensive differential scanning calorimetric (DSC) investigation has been conducted on the precipitation and dissolution behaviour of SiC particulate-reinforced 7091 aluminium. DSC is shown to be a particularly attractive experimental technique for developing new thermal and thermomechanical processes for aluminium-based metal matrix composites. These new processes are necessitated due to the deleterious effects that the SiC reinforcement causes on the aluminium matrix precipitation behaviour and the resultant ductility and fracture toughness properties. In this study the effects of SiC concentration and ageing temperatures, times, and sequences were evaluated. In addition to the unreinforced 7091 alloy, composites containing 10, 20 and 30 vol% particulate SiC were characterized. Identifications of specific phases involved in reactions detected with DSC were achieved by making direct correlations to previously published transmission electron microscopy studies. It was found that the presence of SiC in the aluminium significantly affects the solid state transformation kinetics of the 7091 aluminium matrix. Specifically, increasing the SiC concentration was found to decrease the temperatures at which GPI and GPII zones precipitate at their maximum rates and to increase the temperature at which GPI zones revert at maximum rate. The transition phase, η', and equilibrium phase, η, formation kinetics were observed to be insensitive to SiC concentration. Also, increasing the SiC concentration was seen to decrease the temperature at which the equilibrium phase dissolution occurred at its maximum rate. Transformation mechanics have been proposed which are consistent with these observations.

1. Introduction

Discontinuous ceramic-reinforced metals possessing high specific strength and stiffness have been the object of intense study and development during the 1980s. In particular, SiC-reinforced aluminium materials have demonstrated substantially higher strength and stiffness values than their corresponding unreinforced counterparts. These property improvements are achieved because of the high modulus and strength that is characteristic of the SiC reinforcement. However, these materials have exhibited very poor ductility and fracture toughness. In attempting to improve these properties and also yield even higher levels of strength, considerable effort has been devoted to developing appropriate heat treatment and thermomechanical process procedures for these materials systems. These new procedures are required because the presence of SiC in the aluminium matrix significantly influences the precipitation kinetics and precipitate morphology in the matrix.

Historically, studies involving precipitation characterization in aluminium alloys have used such techniques as electrical resistivity and hardness measurements, X-ray diffraction, and transmission electron microscopy (TEM). However, in recent years, differential scanning calorimetry (DSC) has been used increasingly for these studies [1–10], being particularly useful for assessing kinetic aspects. While DSC has seen considerable use in characterizing unreinforced alloys, relatively little has been documented on use of this powerful method for reinforced metallic composites [11–14].

DSC is a particularly attractive experimental technique for developing new thermal and thermomechanical processes for metal matrix composite (MMC) materials. The effects of numerous temperature, time, and deformation possibilities and combinations can be assessed relatively quickly via DSC experimentation. Specifically, with respect to alternate evaluation tools, DSC has been found to be a preferable technique for aluminium-based MMC materials for the following reasons:

(1) the reinforcement in MMC renders these materials insensitive to detection of microstructural

0022–2461/89 $03.00 + .12

changes via traditional hardness, microhardness, and resistivity measurements;

(2) the DSC apparatus is simple to operate, sample size is small, sample preparation is rapid, and data interpretation is straight-forward. This contrasts to X-ray and TEM techniques that can require costly sample preparation and extensive analysis.

In the present programme, DSC has been used as the primary evaluation method for developing improved processing for particulate SiC-reinforced 7091 aluminium alloy. This alloy was selected for investigation because of its potential for use in high-strength aerospace applications. This MMC system, along with discontinuous SiC-reinforced 2124 aluminium, has been the subject of extensive research recently at the University of Texas at Arlington [11, 14–16]. In these investigations DSC was used both as a screening tool for new process development and a microstructural "fingerprinting" method for isolating specific precipitation reactions. This research resulted in some special processing techniques that significantly improved the low fracture toughness and fatigue crack growth resistance of these MMC systems. This was accomplished by employing schemes which were designed to influence the precipitation of the secondary phases in a more homogeneous manner throughout the matrix. This reference research concentrated mainly on improving ultimate properties, rather than providing complete DSC characterizations of these systems.

The objective of the present programme was thus to develop a full DSC characterization of precipitation reactions in the discontinuous SiC-reinforced 7091 aluminium system, so that DSC experimentation can be used more effectively in tailoring thermal and thermomechanical processes for ultimate properties. The specific variables of most interest included the amount of SiC in the MMC system and processing temperatures, times, and sequences. In order to accomplish this, SiC-reinforcement volume fractions of 10, 20, and 30% were studied, in addition to an unreinforced 7091 aluminium baseline. Identifications of specific phases involved in reactions detected with DSC were achieved by making direct correlations to previously published transmission electron microscopy studies.

2. Experimental procedure

A 7091/SiC composite material was fabricated and donated by DWA Composite Specialities, Inc (Chatsworth, California, USA). The SiC reinforcement was made from abrasive-grade SiC crushed into fine powder and blended mechanically with the proper alloy powder. The mixture was then processed into billets using proprietary powder metallurgy techniques. The billets were extruded into 127 mm wide by 13 mm thick planks. Four different composition composites were received in this extruded plank form: 0, 10, 20 and 30 vol % SiC concentrations. The nominal composition for the 7091 aluminium alloy contains the following weight percentages: 6.5 Zn, 1.5 Cu, 2.5 Mg, 0.4 Co, Al balance.

DSC coupons were manually punched from thin sections, 2.5 mm thick, and ground on one side to provide a flat surface for proper seating in the DSC cell. Selection of DSC coupons for any series of tests was at random throughout the extrusion. A minimum of two DSC scans was performed on each condition. All DSC coupons were punched prior to any heat treatment to eliminate any influences on the precipitation that the punching operation might cause [17, 18].

All DSC coupons were subjected to desired heat treatments prior to DSC evaluation. These heat treatments consisted of selected segments of the precipitation-hardening thermal process routinely given to 7000 series aluminium alloys. This process includes solution treatment, quench and various age segments. The precise heat treatments chosen for the DSC coupons were identical to procedures documented in published TEM precipitation studies of Al–Zn–Mg and Al–Zn–Mg–Cu alloys similar in composition to 7091. This enabled direct correlation of the DSC results with specific precipitation processes occurring during various stages of a typical precipitation-hardening heat treatment. After heat treating, the coupons were stored in a freezer maintained at 0° C until DSC scans could be conducted. Complete details of this work have been documented in earlier work [14].

DSC tests were performed in a DuPont 910 scanning calorimetry cell using a 1090 thermal analyser. Coupons were encapsulated in standard high-purity aluminium sample pans. A similar aluminium sample pan was used as a reference. Each scan was conducted from 30 to 500° C. A dry argon or nitrogen gas purge at 1 litre/min^{-1} was used to limit oxidation reactions. A scanning rate of 20° C min^{-1} was used for all tests. After completion of the DSC scan, the raw heat-flow data were converted to specific heat capacity using techniques developed by DuPont [19–21]. All heat-capacity data were modified to account for the mass fraction of SiC in the composite and to account for the baseline heat capacity of the material [22, 23].

3. Interpretation of precipitation processes via DSC

The generally accepted precipitation sequence for Al–Zn–Mg and Al–Zn–Mg–Cu alloys which were similar in composition to 7091 is:

supersaturated solid solution

→ GPI zones/GPII zones → transition phase η'

→ equilibrium phase η

The first stage in the decomposition of a supersaturated solid solution is the formation of spherical clusters of coherent solute elements. These clusters are typically known as Gunier–Preston or GPI zones [24, 25]. Many investigators have also documented a second zone traditionally referred to as GPII zones [2, 3, 24]. These GPII zones are also thought to be coherent with the matrix, but to consist of clustered vacancies rather than clustered solutes [26]. Upon continued ageing, these coherent zones begin to grow and eventually a partial loss of coherency occurs. This constitutes the formation of the semicoherent transition phase, η'. This phase possesses a defined crystal structure. The presence of this phase in combinatio

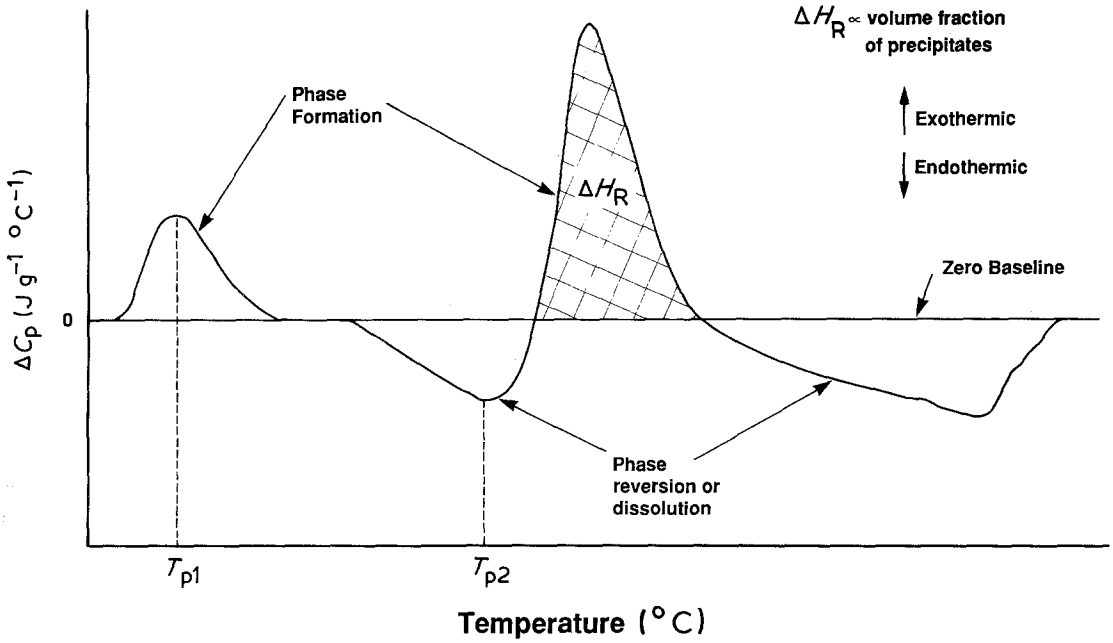

Figure 1 Typical DSC thermogram corrected to zero baseline.

with GPI zones is thought to provide the optimum mechanical strength in 7091-type alloy systems [27].

After further ageing, a complete loss of coherency accompanies development of equilibrium phases in the microstructure. The appearance of η constitutes a loss in mechanical strength. Materials containing significant amounts of η are considered overaged due to the loss in strength.

This decomposition sequence was used to identify a signature DSC thermogram of unreinforced 7091 aluminium. TEM studies were used to specifically age a DSC coupon to obtain a documented microstructure. When the DSC scan was performed, reversion of constituents known to exist in the microstructure produced characteristic endothermic reactions. Furthermore, precipitation of new constituents produced characteristic exothermic reactions. By careful selection of heat treatment prior to the DSC scans, each precipitation reaction could be isolated to produce a characteristic thermal reaction documented by a DSC thermal curve. The details of this procedure are extensive and have been thoroughly documented in prior work [14]; however, a specific example illustrating this method is provided below.

Fig. 1 illustrates a schematic DSC thermogram of a solution treated and quenched aluminium alloy corrected to zero baseline. The reaction peaks represent the thermal events associated with precipitation or dissolution of specific phases in the aluminium matrix. Deviations above the zero baseline are due to

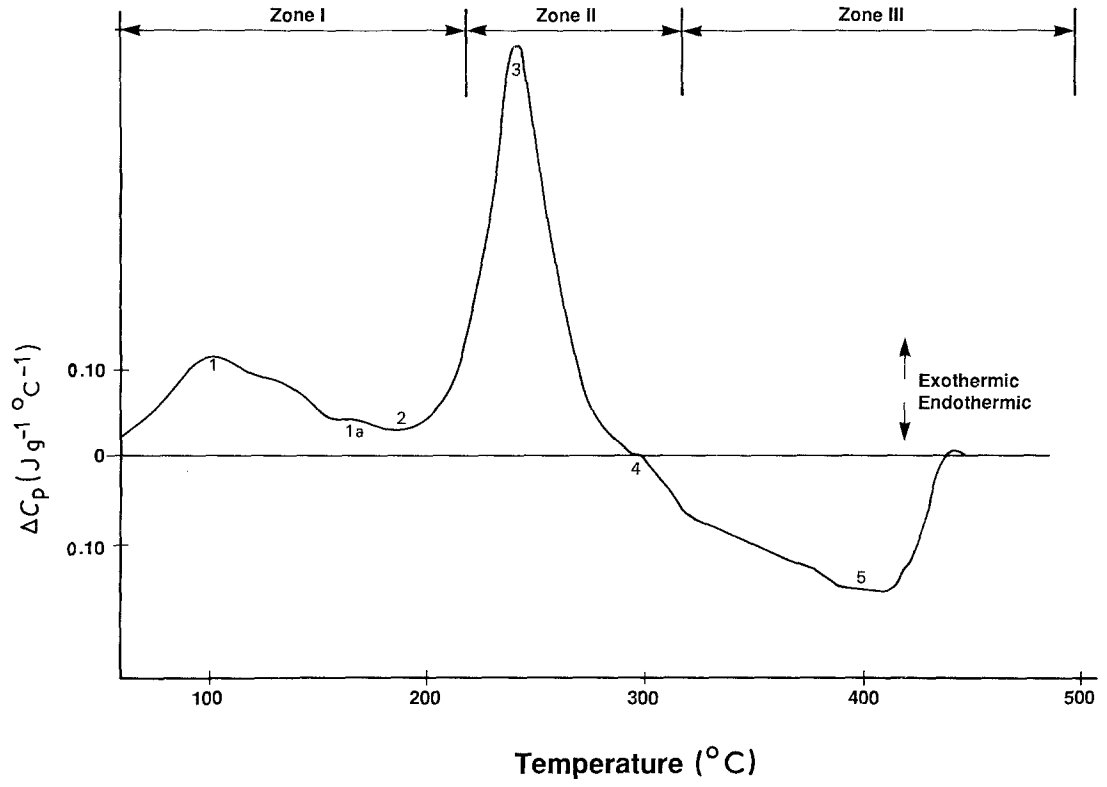

Figure 2 Thermogram of 10 vol % SiC/7091 Al in the as-quenched condition.

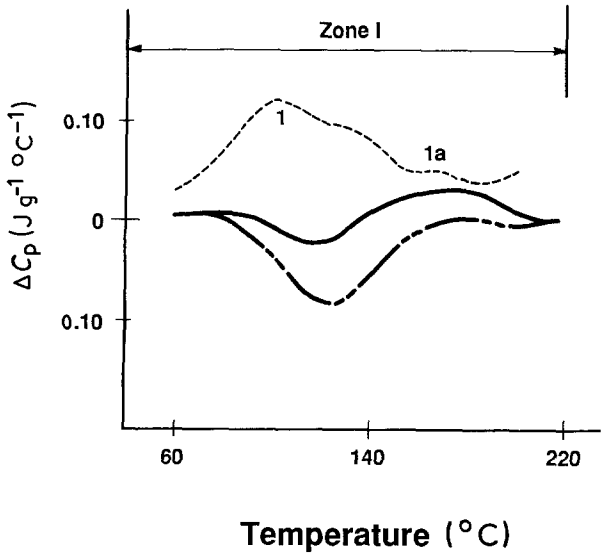

Figure 3 DSC thermogram of 10 vol % SiC/7091 Al. Scan shows the transition of the exotherm, peak 1, associated with GPI-zone formation to a reversion endotherm after ageing at room temperature. Peak 1a is found to remain after ageing for 24 h, suggesting a different zone has formed. (——) 24 h, (- - -) 168 h, (– – –) as-quenched.

exothermic reactions associated with phase formation such as η' precipitation. Deviations below the zero baseline are due to endothermic processes associated with reversion or dissolution of phases, such as GP-zone reversion. The area under the curve defined by the exothermic or endothermic peak and the zero baseline is a measure of the heat of reaction, ΔH, associated with the specific precipitation reaction normalized for the mass of aluminium in the sample. For a specific reaction, ΔH is directly proportional to the volume fraction of precipitate forming or dissolving [5].

An actual DSC thermogram of one of the 7091 based MMC materials (containing 10 vol % SiC) is given in Fig. 2. The DSC coupon had been subjected to a solution treatment at 495° C for 3.5 h followed by quenching into ice-water prior to the DSC run. The thermogram has been divided into three zones. Zone I encompasses the temperature regime from 60 to 220° C. Two exothermic reactions, 1 and 1a, and one endothermic reaction, 2, are observed. Zone II is comprised of the temperature range from 220 to 320° C. In this zone, a large exothermic reaction, 3, and a small exothermic peak imposed on an endothermic reaction, 4, are observed to occur. Zone III ranges from 320 to 500° C and the only reaction occurring in this zone is the large endotherm, 5. To clearly distinguish that the (sometimes superimposed) endothermic and exothermic reactions mentioned above occurred as stated, a progressive sequence of heat treatments was required. Because these heat treatments were identical to those performed for published TEM studies, it was also possible to determine the metallurgical phenomenon associated with each thermal reaction. To illustrate this method, the procedure used to reveal the nature of the phenomenon of peaks 1 and 1a will be reconstructed.

Zone I of Fig. 2 contains two exothermic reactions associated with formation processes (peaks 1 and 1a) and a superimposed endotherm (peak 2) associated with a reversion reaction [1, 15]. To identify the precipitated phases that cause these peaks, a series of room-temperature ageing experiments were conducted in accordance with the TEM study of Honyek *et al.* [2]. The 10 vol % SiC/7091 Al MMC coupons were solution treated, quenched and then aged at room temperature for three different times: as-quenched, 24 h and 168 h. The DSC thermograms for these three coupons are shown in Fig. 3. The absences of peak 1 from the thermograms associated with the 24 and 168 h ageing at room temperature indicates that peak 1 is probably the result of zone formation. In fact, ageing for 168 h produces an endothermic peak in place of peak 1 due to reversion of these low-temperature zones formed prior to the scan [2]. Previous DSC work supported by TEM studies and X-ray small-angle scattering investigations support the conclusion that peak 1 is the result of GP-zone

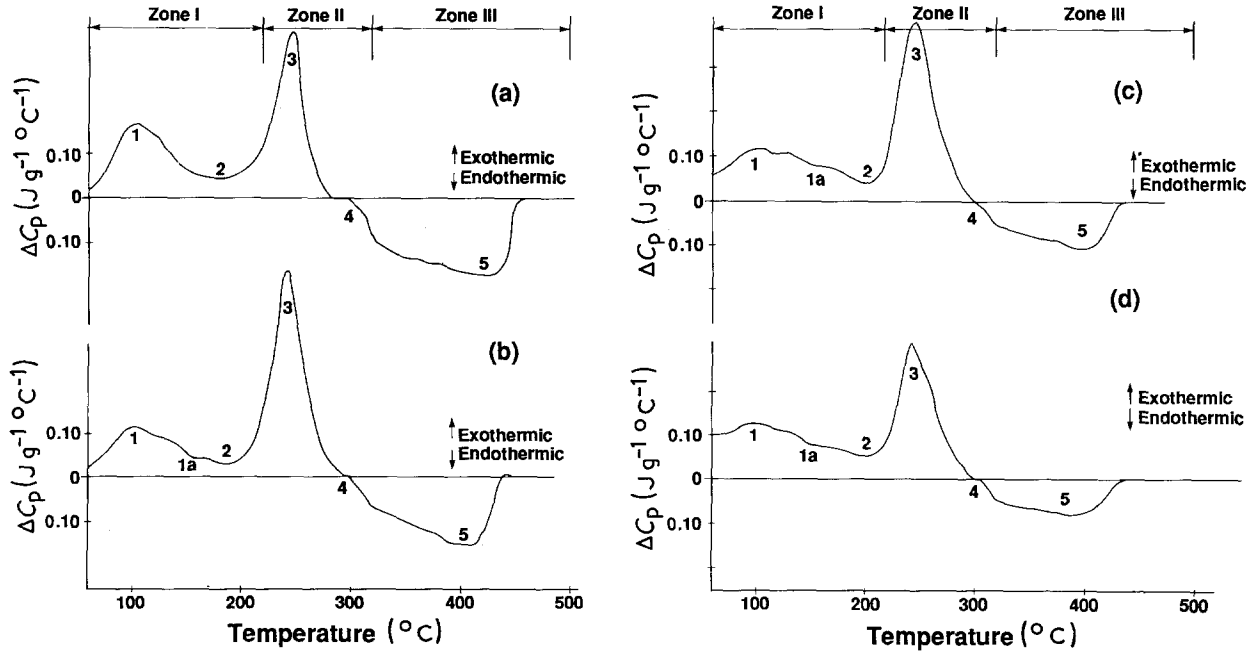

Figure 4 Thermograms of (a) 0 vol % SiC/7091 Al, (b) 10 vol % SiC/7091 Al, (c) 20 vol % SiC/7091 Al and (d) 30 vol % SiC/7091 Al in the as-quenched condition.

formation during the scan of an as-quenched material [2]. Furthermore, an investigation using elastic diffuse neutron scattering detected the presence of GP zones in room-temperature aged material [28]. The second exothermic peak (peak 1a) in Fig. 3 becomes more defined after ageing for 24 h at room temperature. As discussed previously, a second low-temperature zone formation has been observed by many investigators in this type of aluminium alloy [2, 3, 24, 26]. It is highly likely that these GPII zones are the cause of the second exotherm observed. The existence of exothermic peak 1a after an ageing treatment that was designed to precipitate GP-type zones (i.e. 24 h at room temperature) implies that this second zone is more difficult to precipitate, or more soluble than the GPI zones.

The procedure of systematically isolating each thermal-reaction peak associated with documented precipitation reactions as demonstrated above, was employed to interpret all DSC thermograms evaluated in this programme. Once the baseline DSC thermogram of unreinforced 7091 aluminium was fully characterized by this method, the thermograms from 10, 20 and 30 vol % SiC-reinforced 7091 materials could be directly compared to delineate the effects of increasing reinforcement concentration.

4. Kinetic effects of SiC concentration

Fig. 4 shows thermal curves for 0, 10, 20 and 30 vol % SiC-reinforced 7091 aluminium. These thermograms depict the entire decomposition process because the coupons were in a supersaturated state, i.e. solution treated and quenched, just prior to DSC testing. Table I summarizes the precipitation process occurring during each numbered reaction peak in the thermograms.

The specific effects of SiC on the precipitation behaviour of the 7091 matrix are evidenced through DSC experiments by documenting changes in reaction kinetics. The speed with which precipitation or decomposition reactions occur are measured by shifts in the temperatures of the exothermic or endothermic reactions peaks. An exothermic or endothermic reaction exhibits a peak at the temperature at which the reaction is proceeding at its most rapid rate [5, 6, 23, 26]. Fig. 5 illustrates the shifts in the reaction peaks along the temperature axis due to increasing SiC concentration in as-quenched samples. Table II gives the peak-temperature (T_p) shifts from coupons aged to isolate each precipitation reaction using the methods discussed in Section 3.

TABLE I Summary of precipitation reactions associated with each peak in Fig. 4 DSC scans of SiC/7091 Al composites. Materials were in solution-treated and as-quenched condition prior to DSC scans

Peak number	Temperature range (° C)	Material	Reactions occurring during peak
1	60–140	All	GP-zone formation
1a	120–160	All	Vacancy-solute clusters; GP-zone formation
2	160–220	All	GP-zone reversion
3	220–270	A	η' formation; η' dissolution
	220–300	B, C, D	η formation
4	270–320	A	η formation
	300–320	B, C, D	
5	320–445	A	η dissolution
	320–435	B	
	320–430	C, D	

A, unreinforced 7091 Al; B, 10 vol % SiC/7091 Al; C, 20 vol % SiC/7091 Al; D, 30 vol % SiC/7091 Al.

The first reaction shown in Table II is that produced by GPI-zone formation in the matrix. As the SiC concentration increases, a trend of decreasing T_p can be observed. The T_p values shown were derived from thermal scans of coupons in the as-quenched condition. T_p for 0 vol % SiC (or unreinforced aluminium) is 106° C, decreasing down to 98° C as the SiC concentration is increased to 30 vol %.

The next reaction associated with GPII zone formation shows a similar trend. DSC coupons for these T_p values were aged 24 h at room temperature prior to testing in order to differentiate GPII reactions from GPI reactions. T_p for this formation reaction decreases from 175° C for 0 vol % SiC to 170° C for 10 vol % SiC and 148° C for 20 and 30 vol % SiC concentrations.

GPI-zone reversion reactions listed next in Table II appear to respond in direct opposition to the response of GPI-formation reactions as SiC concentration is increased. These coupons were aged at room temperature for 168 h to isolate the reversion reactions from competing reactions prior to testing. At 0 vol % SiC, T_p is 120° C. The 10 and 20 vol % SiC reinforcements increase T_p to 124° C and 30 vol % SiC caused T_p to shift up to 126° C. Although, the 6° C total shift of T_p as SiC concentration increases 30 vol % is small, the span from GPI-zone formation peak to GPI-zone reversion peak is significant. For 0 vol % SiC, this span is 14° C, at 10 vol % SiC the span increases to 22° C, at 20 vol % SiC the span is 24° C, and finally at 30 vol % SiC the span from the GPI-formation peak to the GPI-reversion peak is 28° C. This increasing span of T_p values suggests that the presence of SiC in the aluminium matrix has a profound influence on critical precipitation processes. This in itself reinforces the need to fully characterize and understand the impact of reinforcing agents on fundamental strengthening processes in aluminium alloys.

The next reaction that occurs in the aluminium matrix after GPI and GPII reactions is the simultaneous formation of transition and equilibrium phases of η' and η; and η' dissolution. Delineation of each individual reaction was not possible due to the intimate interaction of the transition and equilibrium phases [14]. However, a very well-defined formation exotherm occurs in coupons in the as-quenched condition prior to testing. The results in Table II indicate that T_p for this reaction appears to be independent of SiC concentrations. The 4° C variation of T_p between 0 and 10 vol %, and 20 and 30 vol % falls within the predetermined experimental tolerance of the T_p measurements (± 2.5° C). Therefore, these reaction kinetics are essentially insensitive to SiC concentration.

The η formation reaction listed next in Table II exhibits a similar insensitivity of T_p to SiC concentration

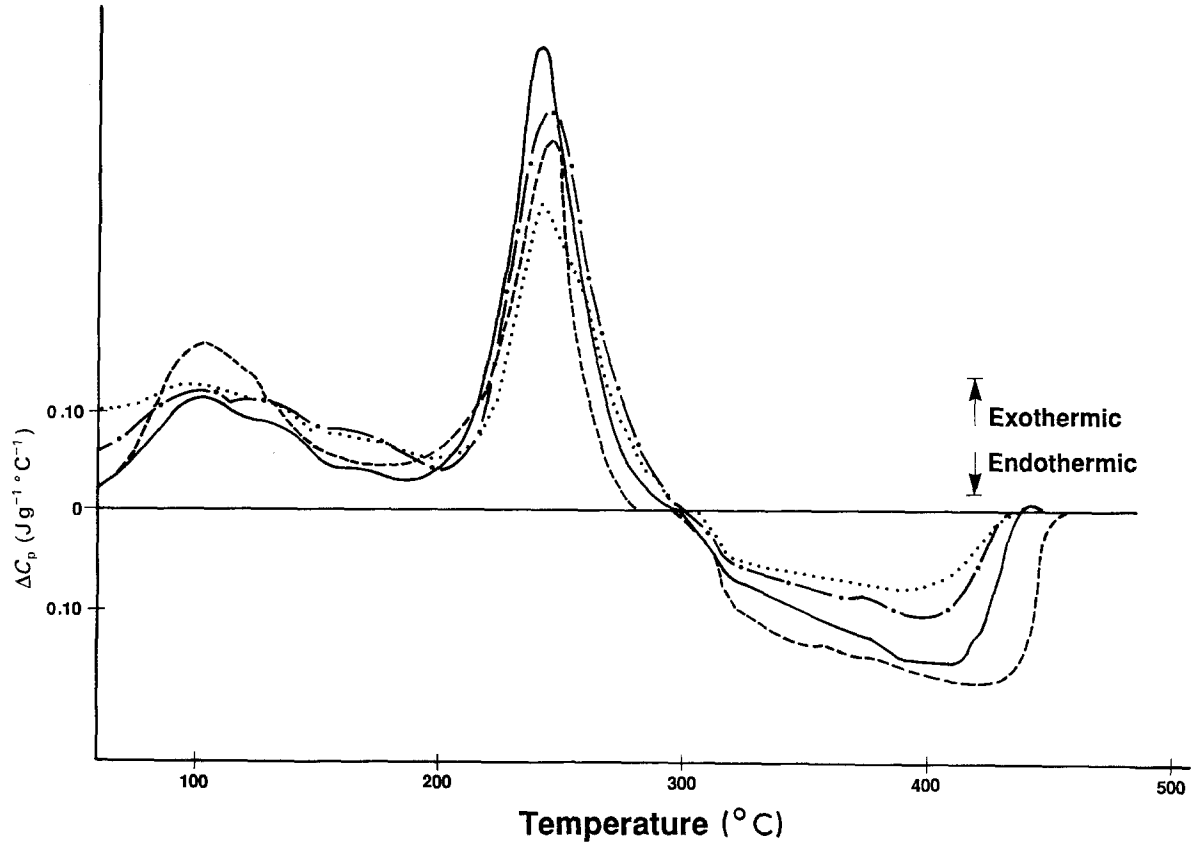

Figure 5 Composite DSC thermograms of (– – –) 0, (——) 10, (–·–·–·–) 20, and (····) 30 vol% SiC and 7091 Al MMC in as-quenched condition, showing shifts of exothermic and endothermic reaction peaks.

to that noted for η' formation. Only a 4° C decrease in T_p is observed as the SiC concentration is increased. Again, this shift in T_p may be considered insignificant. The final decomposition reaction due to dissolution of the equilibrium phase η into solution does show a significant dependence of the reaction kinetics on the SiC concentration. In Table II, the unreinforced alloy shows a T_p of 426° C. A significant shift of T_p down to 406° C is observed when 10 vol% reinforcement is added to the alloy. Further additions of SiC continue to lower T_p to 390° C.

5. SiC effects on precipitation/dissolution mechanisms

The significant alterations in the kinetic behaviour of GPI- and GPII-zone precipitation/reversion reactions and equilibrium η-phase dissolution reactions highlight the need for specialized processing for SiC-reinforced aluminium alloys. Before processing can be developed, an understanding of the mechanisms causing SiC to have such a profound influence on the precipitation kinetics should be pursued.

5.1. GPI- and GPII-zone precipitation

In assessing why increasing the SiC concentration decreases the temperature for maximum GPI-zone formation rate, it may be construed to result from a reduction in the energy barrier required for critical zone nucleation. Two possible mechanisms that may account for SiC reducing the required energy for GP-zone nucleation are: (1) an increase in the internal lattice energy, and (2) a thermal enhancement in solid state diffusion. These mechanisms are inherently interrelated, being directly attributable to the presence of SiC in the aluminium matrix, as discussed below.

The internal lattice energy is increased by an increased dislocation density at the SiC/Al interface. This increased dislocation density has been documented by TEM studies [29, 30]. The dislocation network observed at the interface has been attributed to the

TABLE II Peak temperatures (T_p) for the SiC/7091 Al MMC system. The temperatures were taken from thermograms of materials that had been appropriately aged to isolate the peak under investigation

% SiC	Peak temperature, T_p (° C)					
	GPI-zone formation, from as-quenched material	GPII-zone formation (vacancy-solute clusters), material aged 24 h at room temperature	GPI zone reversion, material aged 168 h at room temperature	η' formation, η' dissolution, η formation from as-quenched material	η formation, material aged 24 h 150° C	η dissolution, from as-quenched material
0	106	175	120	248	294	426
10	102	170	124	244	297	406
20	100	148	124	248	296	400
30	98	148	126	244	298	390

large difference in thermal expansion behaviour of aluminium and SiC [12, 13, 15, 16, 29–31]. When extreme temperature fluctuations occur as in quenching from a solution-treatment temperature, large misfit strains in the aluminium matrix lattice will occur due to the presence of the SiC. This misfit strain will tend to promote strain-induced solid state diffusion of solutes and vacancies to the Al/SiC interface in an effort to reduce the misfit strain in the lattice. Furthermore, the low thermal conductivity of the SiC as compared to the highly conductive aluminium can produce significant microscopic thermal gradients within the material when the material is cooled from elevated temperatures. The matrix adjacent to the SiC reinforcement will tend to be warmer than the aluminium away from the SiC/Al interface. Consequently, solute atoms will migrate to these interfacial zones of higher solubility, their diffusion being enhanced by the increased thermal activation in these regions. On subsequent ageing treatments, then, GPI zones should be observed to form at lower temperatures, their transformation being accelerated by the combined effects noted above.

In a similar fashion, vacancy clustering would be promoted, producing GPII zones at lower ageing temperatures. However, because the exothermic peak associated with GPII zones was observed to shift downward with increase in SiC content to a greater degree than the peak associated with GPI zones, GPII zones appear to be more sensitive to the presence of SiC in the aluminium matrix.

5.2. GPI- and GPII-zone dissolution

It has been theorized that the solute elements and vacancies migrate to the SiC/Al interface due to an increased dislocation network and increased solute solubility caused by a retarded quenching rate at the interface. Therefore, one would expect an excessive concentration of precipitates to be located at or near the SiC/Al interface. This interfacial region, then, must play a prominent role in the decomposition kinetics of an SiC-reinforced aluminium alloy. The heat capacity of SiC is higher than that of aluminium, therefore it would take a greater amount of thermal energy to heat the SiC to a temperature sufficiently high enough to promote GP-zone reversion. Consequently, because the majority of the GP zones are expected to be located close to the SiC/Al interface, they would not tend to revert until enough heat was put into the system to raise the temperature at the interface to promote precipitate reversion. This phenomenon would most likely produce a shift of the GP zone reversion peak in a DSC thermogram to higher temperatures as the SiC concentration in the matrix increases. This is the trend observed for the GPI-zone reversion reaction as noted in Section 4.

5.3. Transition- and equilibrium-phase formations

In contrast to the effect of SiC on the kinetic behaviour of GPI- and GPII-zone formation, the kinetics associated with the transition-phase, η', formation and the equilibrium-phase, η, formation appear to be little affected by the SiC. In prior research, the transition phase, η', has been observed to nucleate heterogeneously on dislocations and other high-energy sites [32]. Complementary to this observation is a high dislocation density associated with the SiC/Al interface [29]. Therefore, one would expect this increased density of nucleation sites to decrease the energy necessary to promote transition phase formation, because the distances for solute diffusion would be reduced. However, this does not appear to be the case. Two pertinent considerations appear relevant when evaluating this apparent contradiction of the results.

1. Transition- and equilibrium-phase reactions may occur at temperatures high enough to produce dislocation annihilation.

2. The transition-phase precipitation may be thermally dependent and not affected by increased strain energy.

If the temperatures involving transition-phase reactions are high enough to allow the dislocations to overcome short-range barriers, they will tend to move to annihilate. In order for this phenomenon to occur during the DSC scan, the dislocations must move at a very rapid rate. However, as temperature increases, the scattering effect of the lattice vibrations would act to slow the dislocation migration down. It is impossible with DSC test results alone to conclude if dislocation annihilation can be disregarded. Utilizing TEM and X-ray techniques with DSC would provide additional information to resolve this effect. If the precipitation kinetics of the transition phase are dictated by thermodynamics, the observed insensitivity of this phase's formation to the presence of SiC is to be expected. For such a situation, phase formation occurs when the free energy of a solution is lowered by the precipitation of a second phase. A combination of free energy and interfacial energy dictates solubility of a particular phase in a host solution at a particular temperature. Furthermore, as the temperature of the solution increases, it begins to play a more dominant role in the free-energy term; therefore, it may be concluded that a certain temperature must be obtained before precipitation of a transition or equilibrium phase can occur, regardless of the density of nucleation sites. This mechanism would, of course, be applicable to the equilibrium-phase formation kinetics, which also appeared to be unaffected by SiC concentration.

The insensitivity of transition- and equilibrium-phase formation kinetics to SiC concentration has been observed by other investigators in a similar alloy system, i.e. Papazian and Adler in a study of 2124 Al with SiC reinforcement [12].

5.4. Equilibrium-phase dissolution

In contrast to the formation reactions just discussed, the dissolution of the equilibrium phase back into solution is accelerated by the presence of SiC in the aluminium matrix. In order for this phenomenon to occur, the SiC reinforcement must be influencing the solubility of the equilibrium phase in the aluminium matrix. As discussed earlier, the solubility of a precipitate in the host solution depends upon the free energy of the solution. These results, showing an

increased solubility of the equilibrium phase in solution, indicate that the overall free energy of the system is lowered more rapidly as the SiC concentration is increased. The mechanism associated with SiC reinforcement causing this behaviour is not clear.

6. Conclusions

A comprehensive calorimetric investigation has been conducted on the precipitation and dissolution behaviour of SiC particulate-reinforced 7091 aluminium. The presence of SiC in the 7091 matrix was observed to significantly affect the solid state transformation kinetics of this aluminium alloy. Specifically, it was found that:

1. increasing SiC concentration decreases the temperatures at which GPI and GPII zones precipitate at their maximum rates;

2. SiC increases the temperature at which GPI zones revert at maximum rate;

3. transition phase, η', and equilibrium phase, η, formation kinetics appear to be insensitive to SiC concentration;

4. increasing SiC concentration decreases the temperature at which the equilibrium phase, η, dissolution occurs at its maximum rate.

Transformation mechanisms have been proposed whose effects are consistent with these observations. The differences in thermal conductivity, thermal expansion and heat capacity between the aluminium matrix and the SiC reinforcement are considered to be the major contributors for the observed changes in precipitation behaviour. With this DSC characterization of the precipitation patterns produced in metal matrix composites, suitable heat treatment and thermomechanical process schemes can more likely be developed that will produce both a strong and damage-tolerant MMC material.

References

1. D. J. SKINNER, R. KER, M. J. KOCZAK and A. LAWLEY, in "Modern Developments in Powder Metallurgy", Vol. 13 Ferrous and Nonferrous Materials, edited by H. H. Hausner, H. W. Antes and G. D. Smith (Metal Powder Industries, Princeton, New Jersey, 1981) p. 483.
2. G. HONYEK, I. KOVACS, J. LENDAVI, NG-HUY-SINH, T. UNGAR, H. LOFFLER and R. GELACH, *J. Mater. Sci.* **16** (1981) 2701.
3. D. S. THOMPSON, in "Thermal Analysis", Vol. 2, edited by R. F. Schwenker Jr and P. D. Garn (Academic, New York, 1969) p. 1147.
4. R. J. LIVAK and J. M. PAPAZIAN, *Scripta Metall.* **18** (1984) 483.
5. R. DeIASI and P. N. ADLER, *Metall. Trans.* **8A** (1977) 1177.
6. W. LACOM, H. P. DEGISCHER, A. M. ZAHRA and C. Y. ZAHRA, *Scripta Metall.* **14** (1980) 253.
7. P. N. ADLER and R. DeIASI, *Metall. Trans.* **8A** (1977) 1185.
8. J. M. PAPAZIAN, *ibid.* **12A** (1981) 269.
9. C. GARCIA-CARDOVILLA and E. LOUIS, *J. Mater. Sci.* **19** (1984) 279.
10. J. M. PAPAZIAN, *Mater. Sci. Eng.* **79** (1986) 97.
11. L. K. AUSTIN and R. D. GOOLSBY, in Proceedings of 31st International SAMPE Symposium, Las Vegas, Nevada, April 1986, edited by J. L. Bauer and R. Dunaetz (SAMPE, Covina, California, 1986).
12. J. M. PAPAZIAN and P. N. ADLER, Grumman Technical Report no. RE-703, Grumman Aerospace Corp., Bethpage, New York, 1985.
13. J. M. PAPAZIAN, Grumman Technical Report no. RE-689, Grumman Aerospace Corp., Bethpage, New York, 1984.
14. J. L. PETTY-GALIS, University of Texas at Arlington, Mechanical Engineering Technical Report no. 86-004 (MS thesis) December 1985.
15. L. K. AUSTIN, University of Texas at Arlington, Mechanical Engineering Technical Report no. 85-005 (MS thesis) August 1985.
16. J. L. PETTY-GALIS and R. D. GOOLSBY, University of Texas at Arlington, Mechanical Engineering Report no. 86-002, August 1986.
17. C. GARCIA-CORDOVILLA and E. LOUIS, *Scripta Metall.* **18** (1984) 291.
18. *Idem, Thermochemica Acta* **93** (1985) 653.
19. R. L. BLAINE, DuPont Co. Application Brief No. TA-88, DuPont Co., Wilmington, Delaware, 1983.
20. D. A. DITMARS, S. ISHIHARA, S. S. CHANG and G. BERNSTEIN, *J. Res. Nat. Bur. Stand.* **87** (1982) 159.
21. DuPont Operators Manual for the 1090B Thermal Analysis System, DuPont Co., Wilmington, Delaware, 1983.
22. S. C. MRAW, *Rev. Sci. Instrum.* **53** (1982) 228.
23. W. P. BRENNAN, PhD dissertation, Princeton University (1971).
24. C. E. LYMAN and J. B. VANDERSANDE, *Metall. Trans.* **7A** (1976) 1211.
25. G. THOMAS and J. NUTTING, *J. Inst. Met.* **88** (1959-60) 81.
26. Z. KATZ and N. RYUM, *Scripta Metall.* **15** (1981) 265.
27. R. NICHOLSON, G. THOMAS and J. NUTTING, *J. Inst. Met.* **87** (1958-59) 429.
28. O. BLASKO, G. ERNST, P. FRATZEL, M. BERNOLE and P. AUGER, *Acta Metall.* **30** (1982) 547.
29. M. VOGELSANG, R. J. ARSENAULT and R. M. FISHER, *Metall. Trans.* **17A** (1986) 379.
30. M. TAYA and T. MORI, *Acta Metall.* **35** (1987) 155.
31. R. J. ARSENAULT and C. S. PANDE, *Scripta Metall.* **18** (1984) 1131.
32. R. M. ALLEN and J. B. VANDER SANDE, *Metall. Trans.* **9A** (1978) 1251.

Received 7 March
and accepted 27 July 1988